The Influence of PMS-Additive on the Electrode/Electrolyte Interfaces in LiFePO 4 /Graphite Li-Ion Batteries

ARTICLE *in* THE JOURNAL OF PHYSICAL CHEMISTRY C · DECEMBER 2013

Impact Factor: 4.77 · DOI: 10.1021/jp4045385

7 AUTHORS, INCLUDING:

Maria Hahlin
Uppsala University
40 PUBLICATIONS **839** CITATIONS
SEE PROFILE

Patrik Johansson
Chalmers University of Technology
113 PUBLICATIONS **2,688** CITATIONS
SEE PROFILE

K. Edström
Uppsala University
219 PUBLICATIONS **4,378** CITATIONS
SEE PROFILE

THE JOURNAL OF PHYSICAL CHEMISTRY C

Article

pubs.acs.org/JPCC

The Influence of PMS-Additive on the Electrode/Electrolyte Interfaces in $LiFePO_4$/Graphite Li-Ion Batteries

K. Ciosek Högström,[†] S. Malmgren,[†] M. Hahlin,[†] H. Rensmo,[‡] F. Thébault,[§] P. Johansson,[§,∥] and K. Edström*[,†,∥]

[†]Department of Chemistry−Ångström Laboratory, Uppsala University, Box 538, SE-751 21 Uppsala, Sweden

[‡]Department of Physics and Materials Science, Uppsala University, Box 516, SE-751 20 Uppsala, Sweden

[§]Department of Applied Physics, Chalmers University of Technology, SE-412 96 Göteborg, Sweden

[∥]Alistore-ERI, 33 rue Saint-Leu, 80039 Amiens cedex, France

Supporting Information

ABSTRACT: The influence of a film-forming additive, propargyl methanesulfonate (PMS), on electrochemical performance and electrode/electrolyte interface composition of $LiFePO_4$/graphite Li-ion batteries has been studied. Combined use of in-house X-ray photoelectron spectroscopy (XPS) and soft and hard X-ray photoelectron spectroscopy (PES) enabled nondestructive depth profiling at four different probing depths in the 2−50 nm range. Cells cycled with PMS and $LiPF_6$ in ethylene carbonate/diethyl carbonate (EC/DEC) were compared to a reference sample cycled without PMS. In the first cycle, PMS cells showed a higher irreversible capacity, which is explained by formation of a thicker solid electrolyte interphase (SEI). After three cycles, the SEI thicknesses were determined to be 19 and 25 nm for the reference and PMS samples, respectively. After the initial cycling, irreversible losses shown by the PMS cells were lower than those of the reference cell. This could be attributed to a different SEI composition and lower differences in the amount of lithium between lithiated and delithiated electrodes for the PMS sample. It was suggested that PMS forms a triple-bonded radical on reduction, which further reacts with the electrolyte. The PMS additive was shown to influence the chemical composition at the positive electrode/electrolyte interface. Thicker interface layers with higher C−O and smaller LiF contributions were formed on $LiFePO_4$ cycled with PMS.

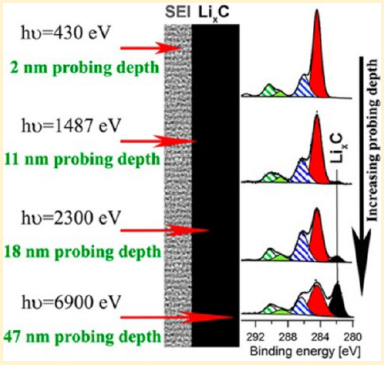

INTRODUCTION

Li-ion batteries have revolutionized the consumer electronics market. At present, they are the most commonly used batteries in low-power applications such as cameras, mobile phones, and laptops. Their usage has been growing rapidly; nowadays, Li-ion batteries are also entering the high-power applications market. They are also an attractive technology for electric vehicles (EV); however, there are some issues that limit their successful implementation. Li-ion batteries are considered too expensive, and their lifetime and safety must be improved. For EVs, lifetimes of more than 10 years are a requirement. For large-scale storage, the lifetime must be even longer.

Most negative electrode materials used in Li-ion batteries operate at voltages that are outside the electrochemical stability window of the most typically used electrolytes (e.g., organic solvents containing a lithium salt). Before the first lithium ions are inserted into negative electrode materials such as graphite, there will be an electrolyte decomposition accompanied by irreversible consumption of some of the lithium ions. This leads to the formation of a solid electrolyte interphase (SEI) and an irreversible loss of capacity because lithium is consumed in the formation of the SEI.[1,2] The SEI covers the surface of the negative electrode particles and ideally protects it from further electrolyte reduction. For graphite, which is used as a negative electrode in commercial batteries, the SEI will also protect particles from cointercalation of solvent molecules and exfoliation.[3] In general, the electrolytes used today will passivate all negative electrode materials that react with lithium below the potential of 0.8 V versus Li^+/Li through the formation of an SEI layer.[2] SEI has been extensively studied, as it has been shown to influence not only the irreversible capacity but also the cyclability, rate capability, and thermal stability of the whole Li-ion battery.[4−6] Furthermore, processes at the negative electrode/electrolyte interface are considered as one of the major sources for a too rapid aging of a Li-ion battery.[7]

Film-forming additives can be used as one way of influencing the composition and properties of the SEI, leading to improved Li-ion battery performances. With few exceptions, the additives that are intended to change the interface chemistry have higher reduction potentials than other electrolyte components. Therefore, they are reduced prior to other electrolyte components. In the early days of Li-ion battery research, it was shown that gaseous species, such as CO_2,[8−10] SO_2,[11,12] and N_2O,[8] improve the electrochemical performance and promote

Received: May 7, 2013
Revised: October 6, 2013

   dx.doi.org/10.1021/jp4045385 | J. Phys. Chem. C XXXX, XXX, XXX−XXX

formation of inorganic films on the graphite anode. None of these additives have been used in commercial batteries; however, the results encouraged interest in functional electrolyte research, and many film-forming additives have since been studied. Among them, a great deal of focus has been put on studying polymerizable monomers with one or more carbon−carbon double bonds. Vinylene carbonate (VC),[13−17] vinyl ethylene carbonate,[18,19] and vinyl acetate[20,21] are just a few examples of investigated compounds. Nowadays, VC is the most well-known SEI precursor. It improves the long-term cycling of the batteries, and it is therfore widely used in commercial Li-ion batteries.

In the present work, we have focused our attention on the film-forming additive propargyl methanesulfonate (PMS). The structural formula for PMS is shown in Figure 1. In an earlier

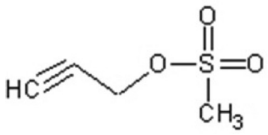

Figure 1. Chemical structure of the PMS additive.

report, it was found that PMS leads to improved cyclability of a $LiCoO_2$/graphite cell and that it prevents graphite exfoliation in propylene carbonate (PC) based electrolytes.[22] It was also shown that the SEI formed when the cell was cycled 50 times with a PMS-PC based electrolyte was thinner than that formed during cycles in an ethylene carbonate (EC) based electrolyte without additive. However, in that study different solvent mixtures were used, and the thicknesses were determined using argon ion etching, which is known to cause decomposition of unstable surface products.[23] There is also a lack of comparison between the PMS-derived SEI with an SEI formed without any additive.

In the present work, graphite/$LiFePO_4$ cells have been cycled and studied with and without the PMS additive using electrochemical and surface characterization techniques. The aim was to determine how the additive would influence the chemical composition of the electrode/electrolyte interface on both graphite and $LiFePO_4$ during the first cycles.

Photoelectron spectroscopy (PES) was used to perform surface depth gradient studies. Soft X-ray PES measurements were performed at the MAX IV Laboratory. Here the outermost part of the SEI surface is studied. XPS studies were performed with an in-house instrument that reaches deeper into the SEI, and the results are comparable to most other studies found in the literature. Hard X-ray PES (HAXPES), which was measured at the Helmholtz Centre Berlin, reach down into the bulk and could thus probe the chemical composition of both the SEI as well as the bulk of graphite or $LiFePO_4$. Excitation energies in a range from 280 to 6900 eV were used, and the probing depth was varied in the 2 to 50 nm range. Hence, we could perform nondestructive depth-profiling of the electrode/electrolyte interfaces. A detailed comparison of the depth gradients in the electrode/electrolyte interfaces of anodes and cathodes from cells cycled with and without PMS additive could thus be obtained.

EXPERIMENTAL METHODS

Battery Preparation. The anode slurry was made from a mixture of 85 wt % potato-shaped graphite (Toyo Tanso), 3 wt % KS6 graphite (Timcal), 2 wt % conductive carbon black (Super P, Erachem Comilog N.V.), and 10 wt % Kynar binder (vinylidene fluoride trifluoroethylene copolymer, Arkema) in *N*-methyl-2-pyrrolidone (NMP) solvent. The cathode slurry consisted of 75 wt % hydrothermally synthesized carbon-coated $LiFePO_4$, 10 wt % conductive carbon black (Super P, Erachem Comilog N.V.), and 15 wt % Kynar binder in NMP solvent. Both slurries were ball-milled. The anode slurry was casted on a copper foil (13 μm thick) and the cathode slurry on an aluminum foil (20 μm thick) using a Hosen pilot line, which allowed the control of a reducible thickness of the coating. The loading of the electrodes was controlled to allow for balancing between the anode and the cathode.

Circular electrodes of a diameter of 2 cm were cut out, moved to an argon-filled glovebox ($\leq$1 ppm H_2O, $\leq$1 ppm O), and dried for at least 5 h at 120 °C in a vacuum oven prior to cell assembly. The standard reference electrolyte was 1 M $LiPF_6$ in ethylene carbonate/diethyl carbonate (EC/DEC) in a 2:1 volume ratio. In addition, 1 wt % of the film-forming additive propargyl methanesulfonate (PMS) was added to some of the electrolytes.

PMS was synthesized following earlier published procedures.[24,25] All chemicals were purchased from Sigma-Aldrich and used without further purification. In detail, a 2 mL solution of propargyl alcohol and a 3.6 mL solution of triethylamine were added to 30 mL of dichloromethane cooled to 0 °C. A 4.1 mL solution of methanesulfonyl chloride was then slowly added over a period of 30 min. The solution was stirred at 0 °C for one hour. The mixture was then extracted with ice water, 10% hydrochloric acid at 0 °C, saturated sodium bicarbonate solution, and brine. Dichloromethane solvent was evaporated under vacuum. The product was a colorless liquid at a 90% yield. Reported ^{1}H NMR:[25] 2.66 ppm, t, 1H, J = 3 Hz (HC≡C−CH_2−O−SO_2−CH_3); 3.10 ppm, s, 3H, (HC≡C−CH_2−O-SO_2−CH_3); 4.86 ppm, d, 2H, J = 3 Hz (HC≡C−CH_2−O−SO_2−CH_3). Experimental ^{1}H NMR: 2.70 ppm, t, 1H; 3.11 ppm, s, 3H; 4.84 ppm, d, 2H. A minor peak at 5.30 ppm in the spectrum indicates traces of dichloromethane remaining in the product; the ^{1}H NMR characterization spectrum of the PMS additive is available as Supporting Information.

Full $LiFePO_4$/graphite cells were assembled within the glovebox in vacuum-sealed polymer-coated aluminum bags. The electrodes were balanced so that the graphite anode had 20% extra capacity.

Electrochemical Measurements. All the electrochemical measurements were carried out in $LiFePO_4$/graphite full cells. Cyclic voltammetry was performed at a 0.01 mV s^{-1} sweep rate and galvanostatic cycling at C/10 between 2.7 and 4.2 V. Samples for interface analysis were collected after the third galvanostatic cycle in charged or discharged state.

PES Measurements and Analysis. Special transfer systems were used to ensure transfer of samples from the glovebox to the PES instruments without contact with air.[26] Caution was taken to avoid radiation damage; most of the measurements were repeated on different batteries in order to obtain reproducible data. All the presented graphs represent measurements performed on unwashed electrodes. However, the measurements have also been performed on electrodes washed with DMC. This was done to keep the advantages of both treatments; unwashed samples guarantee that no SEI components are washed off, whereas washed samples give a useful comparison and guarantee that not only the electrolyte components are being analyzed.

dx.doi.org/10.1021/jp4045385 | J. Phys. Chem. C XXXX, XXX, XXX−XXX

Soft X-ray PES. The most surface sensitive measurements were performed at the I411 beamline at MAX IV Laboratory, the Swedish synchrotron facility. The experiments were made in such a way that electrons emitted from all core levels had similar kinetic energies (~145 eV) and hence similar probing depths. Therefore, C 1s spectra was measured with 430 eV excitation energy (hυ), P 2p spectra with hυ = 280 eV, O 1s spectra with hυ = 680 eV, F 1s spectra with hυ = 835 eV, and S 2p spectra with hυ = 325 eV. C 1s core levels were measured for all chosen excitation energies (besides hυ = 280 eV) to energy calibrate the spectra. The slit through which the X-rays were passing was reduced to less than 1 μm to reduce irradiation-related damage. The electron takeoff angle was 60° defined relative to the surface plane of the sample, and the takeoff direction was collinear with the e-vector of the incident photon beam.

In-House XPS. Measurements were performed on a PHI 5500 system with monochromatized 1486.6 eV Al Kα radiation. The electron takeoff angle was 45° defined relative to the surface plane of the sample.

Hard X-ray PES (HAXPES). More bulk sensitive measurements were performed at the HIKE system, KMC-1 beamline at the BESSY II synchrotron (Berlin, Germany). Two excitation energies were chosen: 2300 eV, first-order radiation monochromatized by Si (111), and 6900 eV, first-order radiation monochromatized by Si (422). For measurements performed at 2300 eV, a 25 μm Be filter was used in order to reduce irradiation-related damage. The 6900 eV radiation was not filtered because of its already lower intensity. The electron takeoff angle was 80° defined relative to the surface plane of the sample, and the takeoff direction was collinear with the e-vector of the incident photon beam.

The combination of synchrotron PES and in-house XPS measurements enabled the performance of a unique non-destructive depth profiling. The excitation energy was varied from 280 to 6900 eV, and samples were thus measured with four different probing depths corresponding to ~2, 11, 18, and 47 nm. The probing depth is defined as 3 times the inelastic mean free path (λ), including 95% of the elastically emitted electrons. Polyethylene inelastic mean free path values are used to estimate the probing depth.[27,28]

Energy calibration was performed with respect to the C−H C 1s core level feature for graphite anode and with respect to the C−C/C−H C 1s core level feature for $LiFePO_4$ cathode, both set to 284.4 eV. PES spectra were fitted in CASA using a 70% Gaussian and 30% Lorentzian mix for the Voigt peak shapes. The lithiated−delithiated carbon anode C 1s peak, termed the Li_xC, was an exception; in that case, an asymmetric peak shape was used.[29] In the presented graphs each spectrum was normalized by the area of the respective core level signal.

Quantifications were discussed using the cross section corrected relative intensities I_j, given by the following equation:

$$I_j = \frac{\frac{A_j}{\sigma_j}}{\sum_i \frac{A_i}{\sigma_i}} \quad (1)$$

where A is the detected core level peak area and σ is the Scofield theoretical photoionization cross section.[30] The SEI thickness d was calculated from the following equation:

$$d = -\ln(I_{Li_xC})\lambda \sin(\theta) \quad (2)$$

where I_{Li_xC} is the relative intensity of the C 1s Li_xC feature, λ the inelastic mean free path, and θ the electron takeoff angle defined relative to the surface plane of the sample. The thickness calculations were based on a model assuming that below a depth d, corresponding to the SEI thickness, the electrode consists of Li_xC only. Thickness calculations are used to give approximate values in order to be able to compare the relative thicknesses in the different cases. The thickness calculations were based on the 2300 eV lithiated graphite data. More details about the experimental part of this study and the performed analysis can be found in previous work performed by some of us.[28]

RESULTS AND DISCUSSION

Electrochemical Studies. Cyclic voltammograms (CVs) for a $LiFePO_4$/graphite cell with PMS additive as well as for a reference cell without additive are shown in Figure 2. As

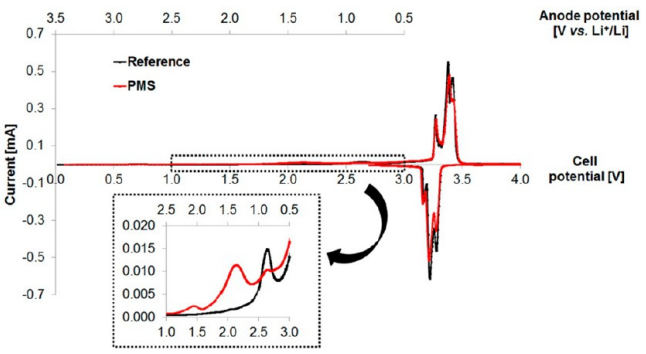

Figure 2. Cyclic voltammogram of a $LiFePO_4$/graphite cell cycled in a standard reference electrolyte and with a PMS additive, recorded with a sweep rate of 0.01 mV s^{-1}.

expected, the typical intercalation processes for the graphite and $LiFePO_4$ are observed in the 3.1−3.5 V range in the CV, whereas peaks corresponding to reduction of electrolyte and SEI formation can be found below 3.0 V. The reference cell (without PMS) exhibited a reductive peak at 2.62 V (0.86 V vs Li^+/Li), which corresponds to solvent reduction. The PMS cell exhibited a small reductive peak at 1.42 V (2.06 V vs Li^+/Li), which may be attributed to reduction of trace oxygen in the electrolyte.[31] The peak at 2.10 V (1.38 V vs Li^+/Li) corresponds to the reduction of the PMS additive, previously reported to take place at 1.24 V versus Li^+/Li.[22] The third peak in the CV of the PMS sample indicates that solvent decomposition (0.86 V vs Li^+/Li) is not fully suppressed, as this is the typical potential where the SEI is formed as indicated by the CV of the reference sample.

Figure 3a shows the three first galvanostatic cycles for $LiFePO_4$/graphite full cells with and without PMS. Both batteries exhibit similar performance. However, the PMS cell shows slightly higher irreversible capacity in the first cycle and slightly lower irreversible capacity in the following cycles. The irreversible capacities for both the PMS cell and the reference cell are plotted in Figure 3b. The higher irreversible capacity in the first cycle for the battery with the PMS additive could indicate that a thicker SEI forms in the PMS cells. The lower irreversible capacity in the following cycles could indicate that the SEI in the PMS cell gives a better long-term stability.

On the basis of these results, we wanted to use a set of PES measurements to better understand the surface chemistry of

dx.doi.org/10.1021/jp4045385 | J. Phys. Chem. C XXXX, XXX, XXX−XXX

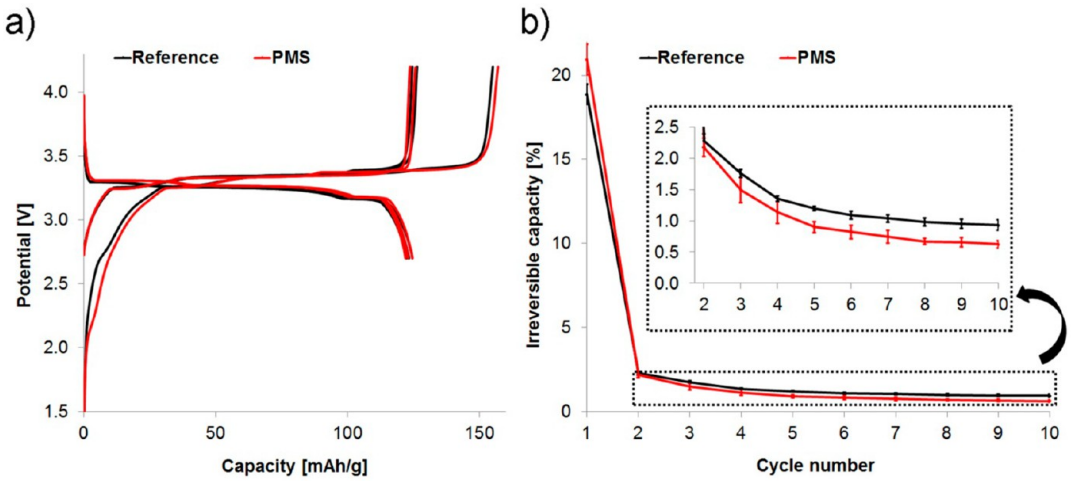

Figure 3. A graphite/$LiFePO_4$ cell cycled with and without 1% PMS additive: comparison of the first three galvanostatic cycles (a) and the change in average irreversible capacity with standard deviation represented by error bars (b).

both the graphite and the $LiFePO_4$ and determine how the surface chemistry would be influenced by electrolytes that differ only in terms of an additive.

Interface Studies. *SEI Thickness in Lithiated Graphite Anode.* The graphite selected for this study is of a standard type with a ~20 μm grain size. We are looking at the complete electrodes, with binder, carbon black additive, and the electroactive material. For the interface analysis the graphite electrodes were stopped after the third galvanostatic cycle in either charged or discharged state.

The PES depth profile (Figure 4) represents lithiated graphite anode from cells cycled in the standard electrolyte, called reference, and in an electrolyte containing the PMS additive. Similar depth profiles have previously been published for cells cycled in the standard electrolyte,[28] but in this study a new set of batteries was measured and an even more detailed depth profiling was made by also including data measured with traditional in-house XPS and by comparing results based on unwashed electrodes to samples that have been washed prior to measurements. In this way important trends could be followed.

The C 1s spectra in the depth profile in Figure 4 show more of the bulk components with probing depth (by increasing the energy of the incoming X-ray). The lithiated carbon Li_xC peak at 282.0 eV in the C 1s spectra becomes clearly visible as the probing depth increases. Cells cycled with PMS additive show a smaller Li_xC intensity, which indicates that the SEI formed is thicker than that of the reference samples. This is based on the measurements showing strong Li_xC signals. The thickness of the SEI was estimated to be 19 and 25 nm for the reference and PMS samples, respectively. This result is in agreement with the electrochemical studies, which indicated that a thicker SEI is formed with the PMS additive.

SEI Composition in Lithiated Graphite Anode. Besides the difference in thickness, similar trends with respect to the C 1s spectral features are observed in the graphite depth profiles for samples cycled in a standard electrolyte and with the PMS additive. We can see that the SEI is not homogeneous, e.g., the C−H contribution (284.4 eV in the C 1s spectra in Figure 4) decreases with probing depth, which indicates that hydrocarbon-containing compounds are more common in the outermost part of the SEI further from the graphite surface.

Turning to the P 2p spectra in Figure 4, we observe SEI compounds containing P−F bonds (at a binding energy of 136.6 eV in the P 2p 3/2 spectra and 2151.9 eV in the P 1s spectra). Moreover, already in the most surface sensitive measurements we observe a small peak at lower binding energies, indicating compounds containing P−O/P═O bonds (at the binding energy 133.7 eV in the P 2p 3/2 spectra and at 2148.5 eV in P 1s). The relative intensity of both, P−F and P−O/P═O features versus the other core levels is decreasing for probing depths corresponding to 11 and 18 nm, indicating that these compounds are found in the outermost part of the SEI. This trend was observed in both unwashed and washed samples; hence, this can not be attributed only to larger amounts of electrolyte residues in the outermost SEI.

In the F 1s spectra shown in Figure 4, small amounts of lithium fluoride, LiF (684.7 eV in F 1s) are detected closer to the bulk material. These amounts are lower than earlier reported for similar graphite/$LiPF_6$ electrolyte studies.[5] The reason for this is probably linked to the improved data acquisition rate which allows better control over the experimental conditions compared to measurements performed 10 years ago. The relative intensity of the LiF feature was found to increase during prolonged measurement time, indicating a slow reaction in the SEI forming the stable compound LiF due to the X-ray exposure used in the experiment.

Some compounds are not detectable when studying the outermost SEI, but when probing deeper into the SEI they become visible. Lithium alkoxide, LiOR (~530.2 eV in O 1s) and lithium oxide, Li_2O (527.6 eV in O 1s), are two examples of compounds that are detected only deeper in the electrode/electrolyte interface close to the bulk material. Li_2O could be formed by reduction of Li_2CO_3 or during reaction of lithiated carbon with air.[26,28] When comparing the contributions of LiOR-species in the O 1s spectra in Figure 4, we note that relatively larger amounts of this compound are observed in the PES measurements of the SEI for the reference electrode compared to an electrode cycled with PMS. However, we have to keep in mind that the SEI is not homogeneous and that the LiOR contribution is observed to increase with probing depth. Because cells cycled with PMS have thicker SEI, we have different sensitivity to the regions closest to the bulk material. We are less sensitive to compounds that are closer to the active material for the PMS sample compared to the reference sample. As a result, the signal from compounds which are preferentially found close to the bulk of graphite, e.g. alkoxide, will be more

dx.doi.org/10.1021/jp4045385 | J. Phys. Chem. C XXXX, XXX, XXX−XXX

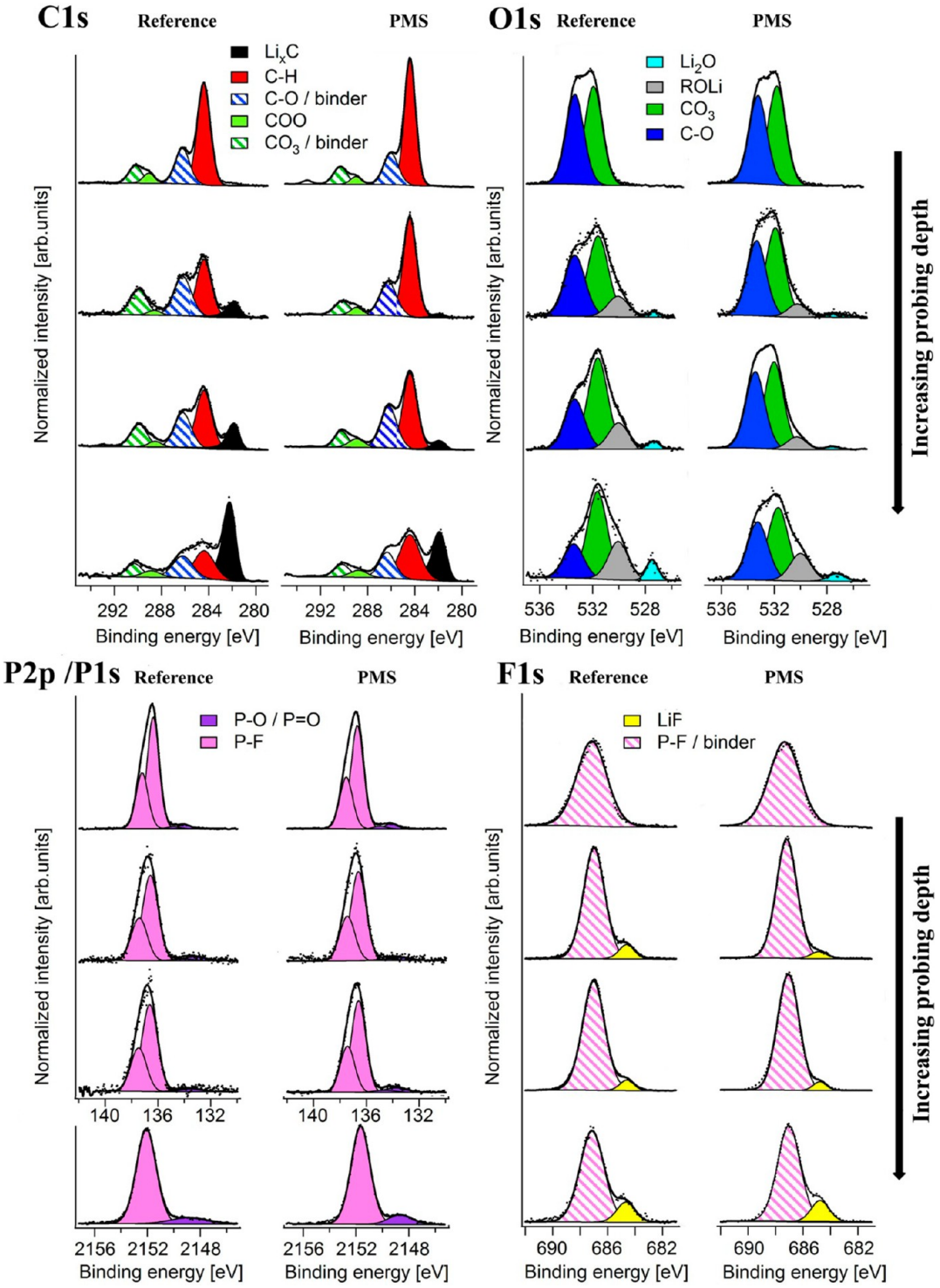

Figure 4. Depth profiling of lithiated graphite electrodes cycled in a standard reference electrolyte and with PMS additive. Probing depth corresponds to ~2, 11, 18, and 47 nm (from top to bottom in each figure).

attenuated in the case of the thicker SEI in the PMS sample. In view of this, it is difficult to compare the amounts of LiOR and Li_2O for the different samples.

In the O 1s spectra (Figure 4), the carbonate feature (~531.8 eV in the O 1s spectra) slightly increases with probing depth for both the reference and the PMS sample. In the reference sample, the contribution from ether-type compounds significantly decreases with probing depth, whereas in the PMS sample the O 1s core level intensity referred to oxygen in C−O bonds (533.4 eV in O 1s) seems to be more constant. To better understand these observations some different reduction mechanisms for EC will be discussed below.

According to the literature, the most commonly suggested EC reduction products are dilithium ethylene dicarbonate $(LiOCO_2CH_2)_2$[32,33] and lithium carbonate (Li_2CO_3).[32,34] It was suggested that $(LiOCO_2CH_2)_2$ is formed by reduction of EC[32,35]

dx.doi.org/10.1021/jp4045385 | J. Phys. Chem. C XXXX, XXX, XXX−XXX

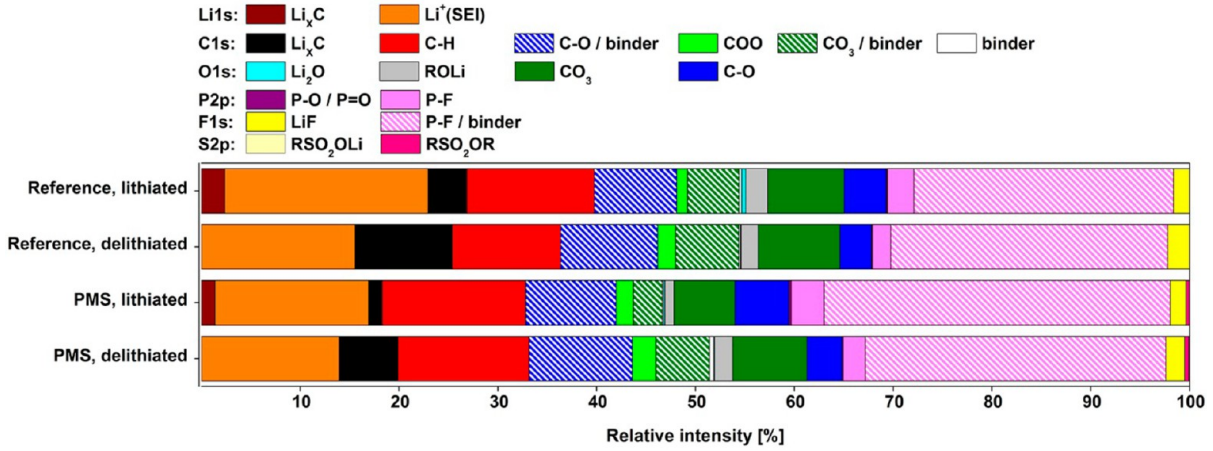

Figure 5. Relative intensities of detected core level peaks referred to different components for lithiated and delithiated graphite cycled with and without PMS additive. Probing depth in the measurements is ~18 nm.

$$2(CH_2O)_2CO + 2e^- + 2Li^+ \rightarrow (LiOCO_2CH_2)_2 + C_2H_4 \quad (3)$$

which has been proposed to further decompose to form inorganic salts by[36]

$$(LiOCO_2CH_2)_2 \rightarrow Li_2CO_3 + C_2H_4 + CO_2 + 1/2O_2 \quad (4)$$

or by electrochemical reduction[5]

$$(LiOCO_2CH_2)_2 + 2Li^+ + 2e^- \rightarrow 2Li_2CO_3 + C_2H_4 \quad (5)$$

Our results of the reference sample show that the core levels representing C−O decrease with probing depth at the same time as the carbonate feature is observed to grow. Taking into consideration that $(LiOCO_2CH_2)_2$ contains both C−O and CO_3 groups, whereas Li_2CO_3 has only carbonate bonds, the observed depth gradients may be related to the fact that more $(LiOCO_2CH_2)_2$ is found in the outermost part of SEI and more Li_2CO_3 deeper in the SEI.

In the PMS sample, the ratio between CO_3 and C−O features is more similar at all the measured probing depths. Together with the significantly higher hydrocarbon intensity in the PMS sample spectra, this indicates that even though the SEI composition seems to be relatively similar in the two types of samples different SEI formation mechanisms and different products are formed on the sample with this additive.

Specific Variations in SEI Composition for Lithiated and Delithiated Graphite Electrodes. To gain more insight into the differences in SEI composition between the reference and PMS samples, lithiated and delithiated graphite electrodes from PMS cells as well as from reference cells were studied and compared.

For both the reference and PMS samples, the Li$_x$C and lithium intensity varies significantly between lithiated and delithiated state, as shown in Figures 5 and 6. According to Figure 5, lithiation is accompanied by higher relative intensity of hydrocarbon and C−O-containing compounds, but slightly higher amounts of P−F and P−O/P═O features also are observed in the charged state. In the depth profiling study we showed that all those compounds are mainly detected in the outermost part of the SEI. This can be interpreted as the outermost part of the SEI "growing" during lithiation of the graphite electrode. It indicates that the SEI is quite dynamically growing and shrinking during intercalation and deintercalation of lithium in graphite after three cycles. Possibly, these changes might also be linked to the irreversible capacity losses.

To give a better description to the differences between the PMS and reference samples, we will here give a detailed analysis of the Li 1s core level spectra of lithiated and delithiated samples, presented in Figure 6. The main peak at ~55.6 eV corresponds to the mixture of various SEI components. In the lithiated state, a peak at ~53.5 eV also can be resolved. On the basis of the difference between the binding energies for the C 1s and Li 1s lithiated carbon features in previously published results,[37] the 53.5 eV feature matches the position of lithiated carbon, Li$_x$C. This is, to our knowledge, the first time that Li 1s spectra of an electrochemically lithiated graphite composite electrode has been detected with a probing depth sufficient to obtain a significant spectral contribution also from the lithiated substrate. The corresponding peak in the C 1s spectra for lithiated carbon Li$_x$C is detected at 282.0 eV (Figure 6).

The difference in the detected amounts of lithium components, as represented in figure 5, between lithiated and delithiated samples, is 3.0% for the PMS samples and 7.4% for the reference samples. The lithiated carbon observed at low binding energy (~53.5 eV in Li 1s) could not fully account for these differences. A major part of the variation, 1.6% for PMS and 5.1% for the reference sample, corresponds to variations in the main peak found at ~55.6 eV in the Li 1s spectra, which refers to the lithium ions present in the SEI and not in the bulk material. As the variation in the Li 1s intensity between lithiated and delithiated electrodes is significantly smaller for the PMS sample, this may be interpreted as the SEI in the PMS sample is more stable than the SEI in the reference sample. The lower irreversible capacity loss seen beyond the first cycle in these cells (Figure 3b) might be related to such increased SEI stability.

It is important to note the small amounts (~0.3%) of detected sulfur in the SEI of graphite samples cycled in the PMS-containing electrolyte. Even smaller amounts of sulfur were detected in a sample soaked with electrolyte (not cycled); in this case, the sulfur signal was barely detectable. In washed, cycled samples, the percentage of sulfur (0.4%) obtained was larger than that in the SEI of the unwashed, cycled samples. This indicates that the sulfur, although in small quantities, is part of the SEI and not only a rest product from the electrolyte.

Decomposition of PMS. Figure 7 shows the depth profile of the S 2p/S 1s spectra of sulfur. The peak at the high binding

dx.doi.org/10.1021/jp4045385 | J. Phys. Chem. C XXXX, XXX, XXX−XXX

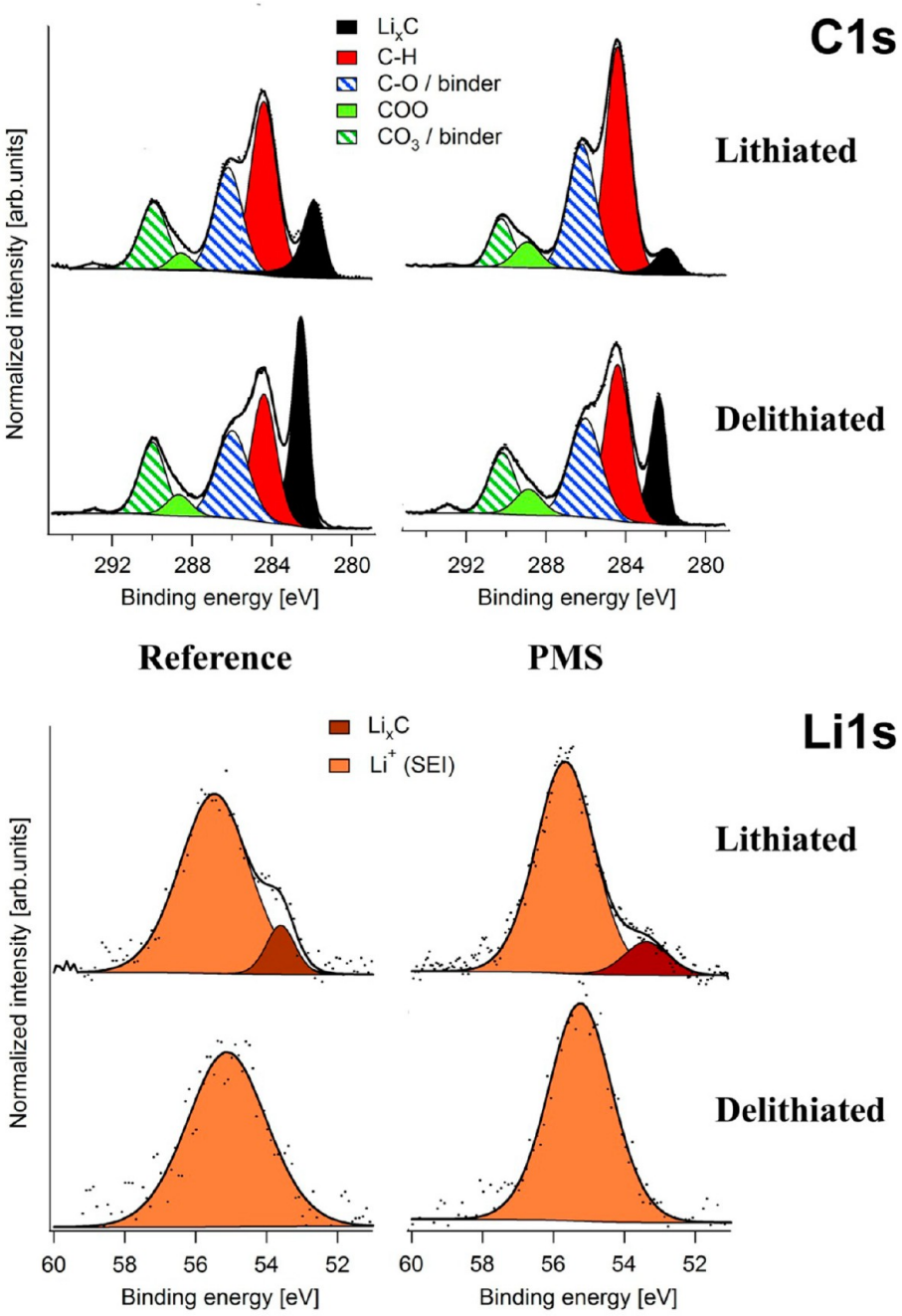

Figure 6. C 1s and Li 1s core level spectra for lithiated and delithiated graphite samples cycled with and without PMS additive. Probing depth ~18 nm.

energy in the S 2p/S 1s spectra has a very similar binding energy to the PMS molecule (S 2p 3/2 168.5 eV, S 1s 2477.5 eV).[38] This indicates that a majority of the sulfur containing product has a similar sulfur environment as the PMS molecule. Such a product could be formed through the, e.g., exchange of propargyl with different hydrocarbon functional groups. The feature at lower binding energy (observed at 166.4 eV for the S 2p 3/2 core level and at 2475.1 eV for S 1s) shows the formation of a new compound in which the sulfur is less positively charged. This compound could be lithium methanesulfonate.

In Figure 8, a suggested reaction scheme for PMS reduction is shown. It was previously suggested that PMS is reduced to form a methanesulfonate anion and a C−C triple-bonded radical.[22] Part of the methanesulfonate anions could react with lithium to form lithium methanesulfonate, which according to the depth profile in Figure 8 is found in the deeper parts of the SEI. Methanesulfonate anions could also react with solvent components to form, for example, lithium methane sulfonate ethyl carbonate. The C−C triple-bonded radical is proposed to polymerize; it could react with EC to form a SEI with higher contributions of hydrocarbon and C−O-containing compounds than found in the reference sample.

Thickness of the Surface Layer on $LiFePO_4$ Cathode. The $LiFePO_4$ sample is a standard compound with high crystallinity and particle size in the 100 nm range. Also in this case the composite electrode including binder, carbon black additive, and the electroactive material was analyzed.

dx.doi.org/10.1021/jp4045385 | J. Phys. Chem. C XXXX, XXX, XXX−XXX

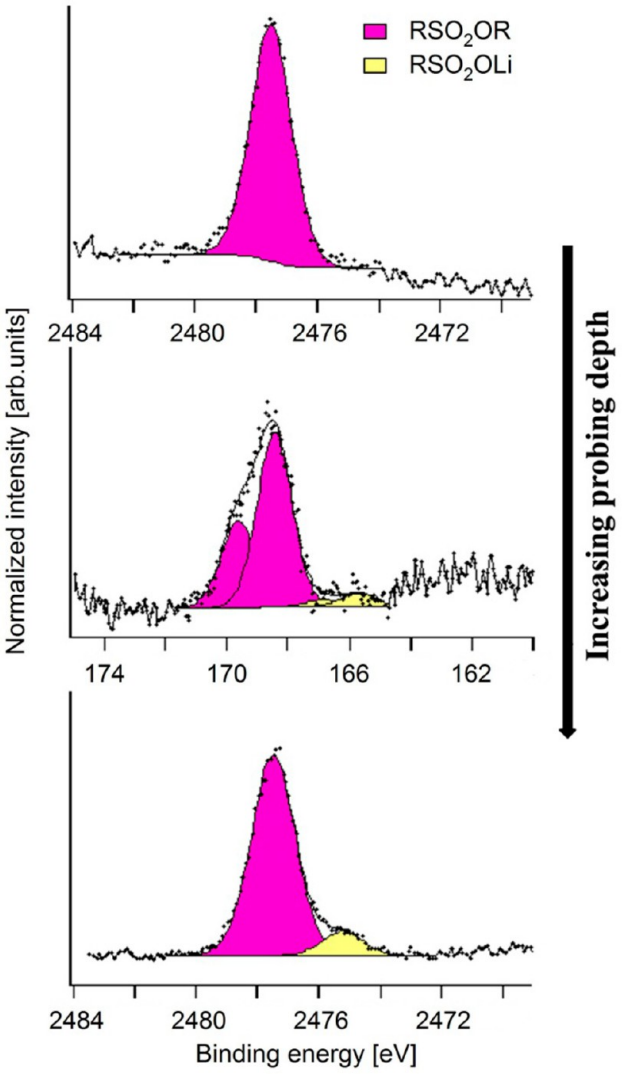

Figure 7. S 1s/S 2p depth profile of lithiated graphite electrode cycled with PMS additive. The probing depths correspond to ~2, 18, and 47 nm.

Figure 9 shows depth profiles of delithiated $LiFePO_4$ electrodes cycled with the standard electrolyte and with PMS additive. In the P 2p spectra for both the reference and the PMS sample, the phosphate feature (133.3 eV in P 2p 3/2, 531.5 eV in O 1s), assigned to the bulk material, is detected already in the most surface sensitive measurements. This confirms that the cathode/electrolyte interface layer is much thinner than the SEI on the negative electrode.[39,40]

The phosphate contribution in the reference sample spectra is clearly more pronounced than that in the PMS sample spectra, which indicates a slightly thicker cathode/electrolyte interface on positive electrodes cycled with PMS. This means that the PMS additive, which is added to facilitate film formation on the graphite, also affects the surface layer on the positive electrode. The main focus of film-forming additive studies has been to improve and investigate their influence on the negative electrode. Only few groups have been investigating the influence of the film-forming additive on positive electrodes. According to previous studies with a different additive, VC,[16,17] the formation of a passivation film was found on $LiCoO_2$, but not on $LiFePO_4$. Here, we show that $LiFePO_4$ cathode also is affected by the film-forming additive PMS.

The cathode/electrolyte interface appears more homogeneous than the SEI formed on the negative electrode. We can see that the C−H/C−C feature (284.4 eV) increases with probing depth. This feature is mainly assigned to the conductive carbon black additive in the composite electrodes and to the carbon coating of $LiFePO_4$ used to enhance the electronic conductivity. Hence, the C−H/C−C signal increases with depth and is therefore more pronounced in the more bulk sensitive measurements. It can, therefore, be attributed to the increased signal from the bulk electrode as the probing depth increases.

Electrode/Electrolyte Interface Composition on $LiFePO_4$ Cathode. Figure 10 shows the relative intensities of core level components detected in the surface layer for delithiated $LiFePO_4$ cycled with and without PMS. Again, samples cycled with the PMS additive show lower relative intensities of the phosphate and C−H/C−C features, which are mainly assigned to the bulk material. However, higher intensities of C−O compounds and slightly larger relative intensities of P−F compounds are seen in the surface of the sample cycled with PMS compared to those of the reference sample. LiF, which is an unwanted compound in the electrode/electrolyte interface because of its low lithium conductivity and higher interface impedance,[4] has a higher intensity in the positive electrode/electrolyte interface on the reference sample.

Figure 11 shows a depth profile of S 2s/S 2p spectra of a delithiated $LiFePO_4$ electrode cycled with the PMS additive. The feature at around 163 eV was sometimes observed in uncycled samples and could be assigned to C−S surface groups. No signs of methanesulfonate formation are observed, and the feature at 168.6 eV could be assigned to the PMS additive as such or to similar sulfonate compounds. It is worth highlighting the low intensity of the peak (0.2% of relative intensity, calculated excluding Fe and Li), which decreases to about half this value for washed electrodes. This could indicate that the

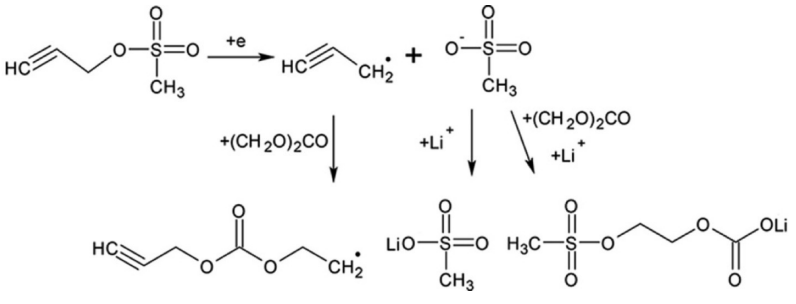

Figure 8. Suggested reaction scheme for PMS-based SEI formation.

dx.doi.org/10.1021/jp4045385 | J. Phys. Chem. C XXXX, XXX, XXX−XXX

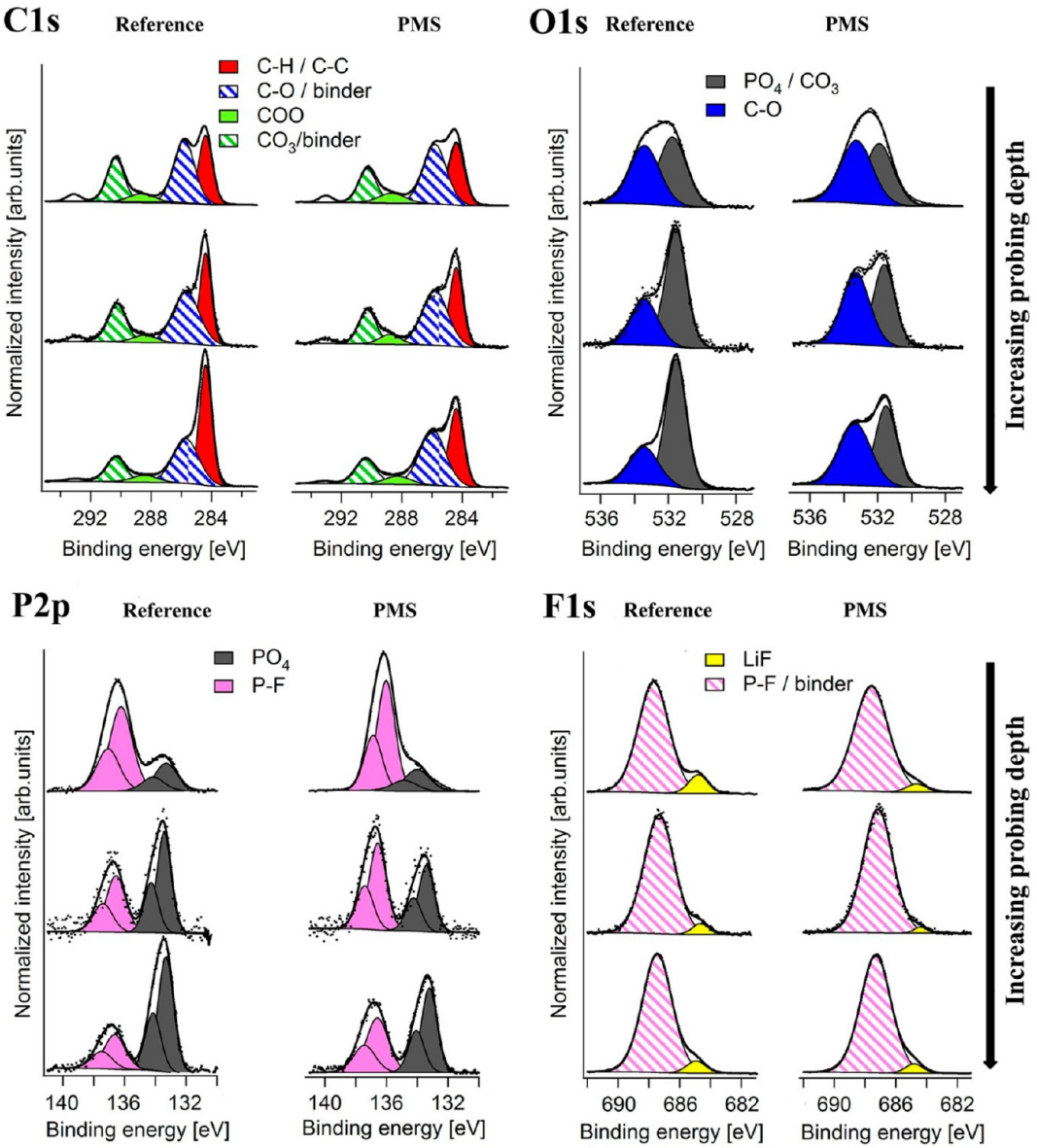

Figure 9. Depth profile of delithiated $LiFePO_4$ electrodes cycled in a standard reference electrolyte and with PMS additive. The probing depths correspond to ~2, 11, and 18 nm.

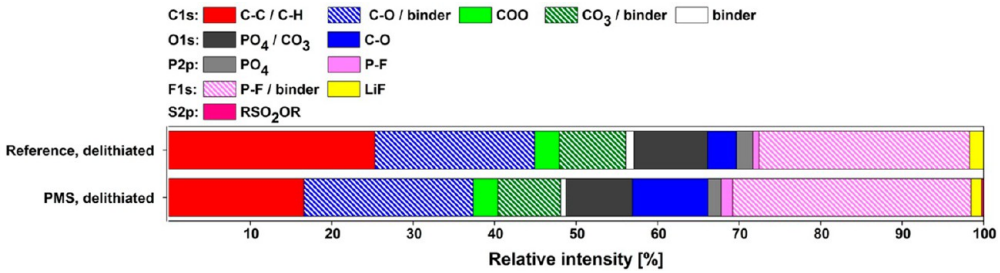

Figure 10. Relative intensities of detected components for delithiated $LiFePO_4$ cycled with and without PMS additive. The graph excludes contribution from lithium and iron. Probing depth ~18 nm.

observed sulfur signal could largely be assigned to electrolyte residuals. Further studies have to be performed to understand the role of the sulfur in PMS on the positive electrode/electrolyte interface.

CONCLUSIONS

This study demonstrates how a combination of nondestructive depth profiling methods, using both soft and hard X-ray PES, give information on the thickness and composition of the surface layers when cycling a battery with the PMS additive.

dx.doi.org/10.1021/jp4045385 | J. Phys. Chem. C XXXX, XXX, XXX–XXX

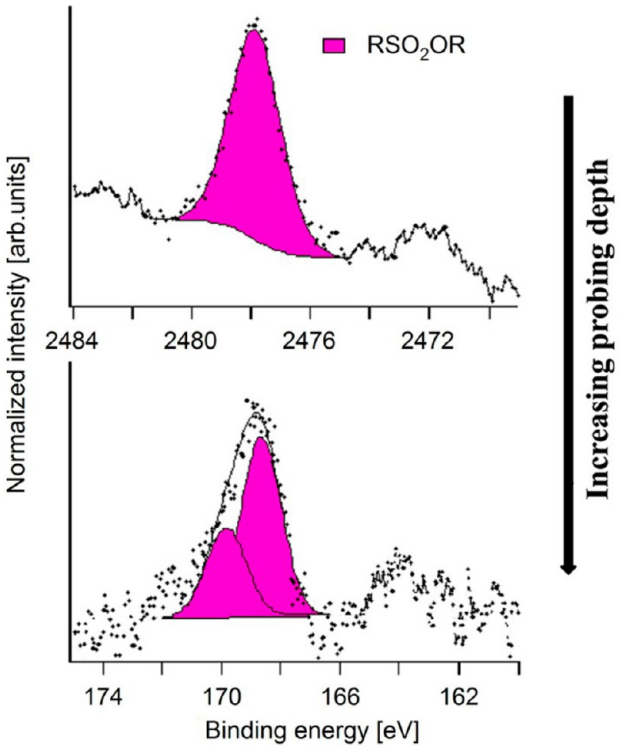

Figure 11. S 1s/S 2p depth profile of a delithiated $LiFePO_4$ electrode cycled with PMS additive. Probing depths correspond to ~2 (top) and 18 nm (bottom).

Our results show that the PMS additive decomposes prior to the electrolyte; however, it does not completely inhibit solvent decomposition. PMS leads to formation of a thicker SEI; after three cycles it was estimated to be 19 and 25 nm thick for reference and PMS samples, respectively. It is suggested that methanesulfonate anions and C−C triple-bonded radicals are formed during PMS reduction. Some of the methanesulfonate anions could form lithium methanesulfonate. The C−C triple-bonded radical polymerizes, and it could react with solvent components to form an SEI with larger amounts of hydrocarbon and a more constant CO_3/C−O ratio for the PMS-cycled electrode compared to that for the reference sample.

The SEI is not stable after three cycles, and during lithiation further electrolyte decomposition takes place for both reference and PMS samples, respectively. When cycling is performed with the standard electrolyte, these processes involve changes in lithium intensity between lithiated and delithiated graphite electrodes that are larger than those in the case of the PMS samples. This accumulation of lithium components could explain the higher irreversible capacity for the reference sample.

The positive electrode/electrolyte interface also is influenced by the PMS additive. A thicker electrode/electrolyte interface with higher contribution of C−O and smaller amount of LiF is found on the $LiFePO_4$ cathode cycled in the PMS-containing electrolyte. There were no signs of PMS decomposition on the positive electrode. Further studies have to be performed to understand the influence of the additive on interfacial properties of the positive electrode.

This study not only provides a better understanding of the influence of PMS additive on Li-ion battery interfaces but also demonstrates a new, powerful technique for comparing samples with different SEI compositions. Compared to measurements performed at only one probing depth or using more destructive methods for depth-profiling such as Ar^+ etching, nondestructive depth profiling using both soft and hard X-ray PES gives an increased and more reliable understanding of depth gradients present in the electrode/electrolyte interface.

■ ASSOCIATED CONTENT

Supporting Information

^1H NMR characterization spectrum of the PMS additive. This material is available free of charge via the Internet at http://pubs.acs.org.

■ AUTHOR INFORMATION

Corresponding Author

*Box 538, SE-751 21 Uppsala, Sweden. Tel: +46 18 471 3713. E-mail: kristina.edstrom@kemi.uu.se.

Notes

The authors declare no competing financial interest.

■ ACKNOWLEDGMENTS

This work was funded by the Swedish Hybrid Vehicle Centre (SHC) and the Swedish Energy Agency (STEM), with additional funding for F.T. from Ångpanneföreningens Forskningsstiftelse, which all are gratefully acknowledged. We are thankful to Leif Nyholm, Torbjörn Gustafsson, Stevén Renault, Bertrand Philippe at Uppsala University, Mihaela Gorgoi at the Helmholtz Centre Berlin Bessy, and Susanne Wilken at Chalmers for useful discussions and support.

■ REFERENCES

(1) Peled, E. The Electrochemical Behavior of Alkali and Alkaline Earth Metals in Nonaqueous Battery Systems—The Solid Electrolyte Interphase Model. *J. Electrochem. Soc.* **1979**, *126*, 2047−2051.

(2) Fong, R.; von Sacken, U.; Dahn, J. R. Studies of Lithium Intercalation into Carbons Using Nonaqueous Electrochemical Cells. *J. Electrochem. Soc.* **1990**, *137*, 2009−2013.

(3) Nazri, G. A.; Pistoia, G. Lithium Batteries: Science and Technology. In *Lithium Batteries: Science and Technology*; Springer: New York, 2003; Vol. *49*.

(4) Andersson, A. M.; Edström, K. Chemical Composition and Morphology of the Elevated Temperature SEI on Graphite. *J. Electrochem. Soc.* **2001**, *148*, A1100−A1109.

(5) Andersson, A. M.; Herstedt, M.; Bishop, A. G.; Edström, K. The Influence of Lithium Salt on the Interfacial Reactions Controlling the Thermal Stability of Graphite Anodes. *Electrochim. Acta* **2002**, *47*, 1885−1898.

(6) Verma, P.; Maire, P.; Novák, P. A Review of the Features and Analyses of the Solid Electrolyte Interphase in Li-Ion Batteries. *Electrochim. Acta* **2010**, *55*, 6332−6341.

(7) Vetter, J.; Novák, P.; Wagner, M. R.; Veit, C.; Möller, K.-C.; Besenhard, J. O.; Winter, M.; Wohlfahrt-Mehrens, M.; Vogler, C.; Hammouche, A. Ageing Mechanisms in Lithium-Ion Batteries. *J. Power Sources* **2005**, *147*, 269−281.

(8) Besenhard, J. O.; Wagner, M. W.; Winter, M.; Jannakoudakis, A. D.; Jannakoudakis, P. D.; Theodoridou, E. Inorganic Film-Forming Electrolyte Additives Improving the Cycling Behaviour of Metallic Lithium Electrodes and the Self-Discharge of Carbon-Lithium Electrodes. *J. Power Sources* **1993**, *43−44*, 413−420.

(9) Chusid, O.; Ein Ely, Y.; Aurbach, D.; Babai, M.; Carmeli, Y. Electrochemical and Spectroscopic Studies of Carbon Electrodes in Lithium Battery Electrolyte Systems. *J. Power Sources* **1993**, *43−44*, 47−64.

(10) Aurbach, D.; Ein-Eli, Y.; Chusid, O.; Carmeli, Y.; Babai, M.; Yamin, H. The Correlation Between the Surface Chemistry and the Performance of Li-Carbon Intercalation Anodes for Rechargeable

"Rocking-Chair" Type Batteries. *J. Electrochem. Soc.* **1994**, *141*, 603–611.
(11) Ein-Eli, Y.; Thomas, S. R.; Koch, V. R. New Electrolyte System for Li-Ion Battery. *J. Electrochem. Soc.* **1996**, *143*, L195–L197.
(12) Ein-Eli, Y.; Thomas, S. R.; Koch, V. R. The Role of SO_2 as an Additive. *J. Electrochem. Soc.* **1997**, *144*, 1159–1165.
(13) Aurbach, D.; Gamolsky, K.; Markovsky, B.; Gofer, Y.; Schmidt, M.; Heider, U. On the Use of Vinylene Carbonate (VC) as an Additive to Electrolyte Solutions for Li-Ion Batteries. *Electrochim. Acta* **2002**, *47*, 1423–1439.
(14) Herstedt, M.; Andersson, A. M.; Rensmo, H.; Siegbahn, H.; Edström, K. Characterisation of the SEI Formed on Natural Graphite in PC-Based Electrolytes. *Electrochim. Acta* **2004**, *49*, 4939–4947.
(15) Herstedt, M.; Rensmo, H.; Siegbahn, H.; Edström, K. Electrolyte Additives for Enhanced Thermal Stability of the Graphite Anode Interface in a Li-Ion Battery. *Electrochim. Acta* **2004**, *49*, 2351–2359.
(16) El Ouatani, L.; Dedryvère, R.; Siret, C.; Biensan, P.; Reynaud, S.; Iratçabal, P.; Gonbeau, D. The Effect of Vinylene Carbonate Additive on Surface Film Formation on Both Electrodes in Li-Ion Batteries. *J. Electrochem. Soc.* **2009**, *156*, A103.
(17) El Ouatani, L.; Dedryvère, R.; Siret, C.; Biensan, P.; Gonbeau, D. Effect of Vinylene Carbonate Additive in Li-Ion Batteries: Comparison of $LiCoO_2$/C, $LiFePO_4$/C, and $LiCoO_2/Li_4Ti_5O_{12}$ Systems. *J. Electrochem. Soc.* **2009**, *156*, A468.
(18) Hu, Y.; Kong, W.; Wang, Z.; Li, H.; Huang, X.; Chen, L. Effect of Morphology and Current Density on the Electrochemical Behavior of Graphite Electrodes in PC-Based Electrolyte Containing VEC Additive. *Electrochem. Solid-State Lett.* **2004**, *7*, A442.
(19) Chen, G.; Zhuang, G. V.; Richardson, T. J.; Liu, G.; Ross, P. N. Anodic Polymerization of Vinyl Ethylene Carbonate in Li-Ion Battery Electrolyte. *Electrochem. Solid-State Lett.* **2005**, *8*, A344.
(20) Yoshitake, H.; Abe, K.; Kitakura, T.; Gong, J. B.; Lee, Y. S.; Nakamura, H.; Yoshio, M. The Effect of Nano-Sized SEI Film Formed by Vinyl Acetate Additive for Li-Ion Batteries. *Chem. Lett.* **2003**, *32*, 1–2.
(21) Abe, K.; Yoshitake, H.; Kitakura, T.; Hattori, T.; Wang, H.; Yoshio, M. Additives-Containing Functional Electrolytes for Suppressing Electrolyte Decomposition in Lithium-Ion Batteries. *Electrochim. Acta* **2004**, *49*, 4613–4622.
(22) Abe, K.; Hattori, T.; Kawabe, K.; Ushigoe, Y.; Yoshitake, H. Functional Electrolytes. *J. Electrochem. Soc.* **2007**, *154*, A810.
(23) Andersson, A. M.; Henningson, A.; Siegbahn, H.; Jansson, U.; Edström, K. Electrochemically Lithiated Graphite Characterised by Photoelectron Spectroscopy. *J. Power Sources* **2003**, *119–121*, 522–527.
(24) Crossland, R. K.; Servis, K. L. A Facile Synthesis of Methanesulfonate Esters. *J. Org. Chem.* **1970**, *35*, 3195–3196.
(25) Jackson, W.; Perlmutter, P.; Smallridge, A. The Stereochemistry of Organometallic Compounds. XXXII. Hydrocyanation of Derivatives of Amino Alkynes. *Aust. J. Chem.* **1985**, *41*, 1201–1208.
(26) Malmgren, S.; Ciosek, K.; Lindblad, R.; Plogmaker, S.; Kühn, J.; Rensmo, H.; Edström, K.; Hahlin, M. Consequences of Air Exposure on the Lithiated Graphite SEI. *Electrochim. Acta* **2013**, *105*, 83–91.
(27) Painter, L. R.; Arakawa, E. T.; Williams, M. W.; Ashley, J. C. Optical Properties of Polyethylene: Measurement and Applications. *Radiat. Res.* **1980**, *83*, 1–18.
(28) Malmgren, S.; Ciosek, K.; Hahlin, M.; Gustafsson, T.; Gorgoi, M.; Rensmo, H.; Edström, K. Comparing Anode and Cathode Electrode/Electrolyte Interface Composition and Morphology Using Soft and Hard X-Ray Photoelectron Spectroscopy. *Electrochim. Acta* **2013**, *97*, 23–32.
(29) Biesinger, M. C. X-ray Photoelectron Spectroscopy (XPS) Reference Pages. http://xpsfitting.blogspot.com/2008/12/graphite.html (accessed Apr 26, 2013).
(30) Scofield, J. H. *Theoretical Photoionization Cross Sections from 1 to 1500 keV*; Lawrence Livermore Laboratory, University of California: Livermore, CA, 1973; Vol. *257*.
(31) Balbuena, P. B.; Wang, Y. Lithium-Ion Batteries Solid-Electrolyte Interphase. In *Lithium-Ion Batteries Solid-Electrolyte Interphase*; Imperial College Press: London, 2004.
(32) Wang, Y.; Nakamura, S.; Ue, M.; Balbuena, P. B. Theoretical Studies to Understand Surface Chemistry on Carbon Anodes for Lithium-Ion Batteries: Reduction Mechanisms of Ethylene Carbonate. *J. Am. Chem. Soc.* **2001**, *123*, 11708–18.
(33) Yang, C. R.; Wang, Y. Y.; Wan, C. C. Composition Analysis of the Passive Film on the Carbon Electrode of a Lithium-Ion Battery with an EC-Based Electrolyte. *J. Power Sources* **1998**, *72*, 66–70.
(34) Kim, S.-P.; van Duin, A. C. T.; Shenoy, V. B. Effect of Electrolytes on the Structure and Evolution of the Solid Electrolyte Interphase (SEI) in Li-Ion Batteries: A Molecular Dynamics Study. *J. Power Sources* **2011**, *196*, 8590–8597.
(35) Aurbach, D.; Levi, M. D.; Levi, E.; Schechter, A. Failure and Stabilization Mechanisms of Graphite Electrodes. *J. Phys. Chem. B* **1997**, *101*, 2195–2206.
(36) Tasaki, K.; Goldberg, A.; Lian, J.-J.; Walker, M.; Timmons, A.; Harris, S. J. Solubility of Lithium Salts Formed on the Lithium-Ion Battery Negative Electrode Surface in Organic Solvents. *J. Electrochem. Soc.* **2009**, *156*, A1019–A1027.
(37) Wertheim, G. K.; Van Attekum, P. M. T. M.; Basu, S. Electronic Structure of Lithium Graphite. *Solid State Commun.* **1980**, *33*, 1127–1130.
(38) Lindberg, B. J.; Hamrin, K.; Johansson, G.; Gelius, U.; Fahlman, A.; Nordling, C.; Siegbahn, K. Molecular Spectroscopy by Means of ESCA II. *Phys. Scr.* **1970**, *1*, 286–298.
(39) Herstedt, M.; Stjerndahl, M.; Nytén, A.; Gustafsson, T.; Rensmo, H.; Siegbahn, H.; Ravet, N.; Armand, M.; Thomas, J. O.; Edström, K. Surface Chemistry of Carbon-Treated $LiFePO_4$ Particles for Li-Ion Battery Cathodes Studied by PES. *Electrochem. Solid-State Lett.* **2003**, *6*, A202–A206.
(40) Dedryvère, R.; Maccario, M.; Croguennec, L.; Le Cras, F.; Delmas, C.; Gonbeau, D. X-Ray Photoelectron Spectroscopy Investigations of Carbon-Coated $LixFePO_4$ Materials. *Chem. Mater.* **2008**, *20*, 7164–7170.